Chilean flat slab subduction controlled by overriding plate thickness and trench rollback

Article *in* Geology · January 2012

DOI: 10.1130/G32543.1

3 authors:

vlad constantin Manea
Universidad Nacional Autónoma de México
93 PUBLICATIONS **1,680** CITATIONS
SEE PROFILE

Marta Perez-Gussinye
Universität Bremen
70 PUBLICATIONS **1,789** CITATIONS
SEE PROFILE

Marina Manea
Universidad Nacional Autónoma de México
76 PUBLICATIONS **1,051** CITATIONS
SEE PROFILE

Geology

Chilean flat slab subduction controlled by overriding plate thickness and trench rollback

Vlad C. Manea, Marta Pérez-Gussinyé and Marina Manea

Geology 2012;40;35-38
doi: 10.1130/G32543.1

Notes

Chilean flat slab subduction controlled by overriding plate thickness and trench rollback

Vlad C. Manea[1]*, Marta Pérez-Gussinyé[2], and Marina Manea[1]
[1]Computational Geodynamics Laboratory, Centro de Geociencias, Campus Juriquilla, Universidad Nacional Autónoma de México, Querétaro, México
[2]Department of Earth Sciences, Royal Holloway, University of London, Egham Hill, TW20 0EX Egham, UK

ABSTRACT

How flat slab geometries are generated has been long debated. It has been suggested that trenchward motion of thick cratons in some areas of South America and Cenozoic North America progressively closed the asthenospheric wedge and induced flat subduction. Here we develop time-dependent numerical experiments to explore how trenchward motion of thick cratons may result in flat subduction. We find that as the craton approaches the trench and the wedge closes, two opposite phenomena control slab geometry: the suction between ocean and continent increases, favoring slab flattening, while the mantle confined within the closing wedge dynamically pushes the slab backward and steepens it. When the slab retreats, as in the Peru and Chile flat slabs, the wedge closure rate and dynamic push are small and suction forces generate, in some cases, flat subduction. We model the past 30 m.y. of subduction in the Chilean flat slab area and demonstrate that trenchward motion of thick lithosphere, 200–300 km, currently ~700–800 km away from the Peru-Chile Trench, reproduces a slab geometry that fits the stress pattern, seismicity distribution, and temporal and spatial evolution of deformation and volcanism in the region. We also suggest that varying trench kinematics may explain some differing slab geometries along South America. When the trench is stationary or advances, the mantle flow within the closing wedge strongly pushes the slab backward and steepens it, possibly explaining the absence of flat subduction in the Bolivian orocline.

INTRODUCTION

Flat slab geometries have been commonly attributed to the extra buoyancy provided by the subduction of young oceanic lithosphere, as suggested for Alaska (Jarrard, 1986), or anomalously thick crust of aseismic ridges, as proposed for South America (e.g., Gutscher et al., 2000). While this explanation may hold when the overriding plate is oceanic, where flat subduction occurs at depths of <~100 km, it is problematic in the flat subduction zones of South America, where the slab entrance angle is normal and flattening only occurs at depths of ≥100 km and extends for hundreds of kilometers inland (Fig. 1). At these depths, the light, thick basaltic crust should transform into denser, heavy eclogite, therefore negating the buoyancy required for flattening, unless basalt remains metastable at larger temperatures and depths (van Hunen et al., 2004). In addition, recent analogue and numeric experiments show that moderate-sized buoyant ridges, such as those observed today on the Nazca plate, are not able to induce flat slab segments of the dimensions observed in South America (Martinod et al., 2005; Gerya et al., 2009). Although a spatial correlation exists between the flat slab areas and the locations of aseismic ridges (the Nazca and Juan Fernandez Ridges), not all aseismic ridges subducting beneath South America spatially correlate with flat subduction segments (Fig. 1; Skinner and Clayton, 2010). Also, the Iquique Ridge is as thick as the Juan Fernandez Ridge (Tassara et al., 2006), yet subducts beneath the Central Andes where the subduction angle is normal (Fig. 1). Moreover, subduction of the Juan Fernandez Ridge during the Late Miocene did not produce any flat slab segment (Martinod et al., 2010). Other significant examples of aseismic ridges not associated with flat subduction include the

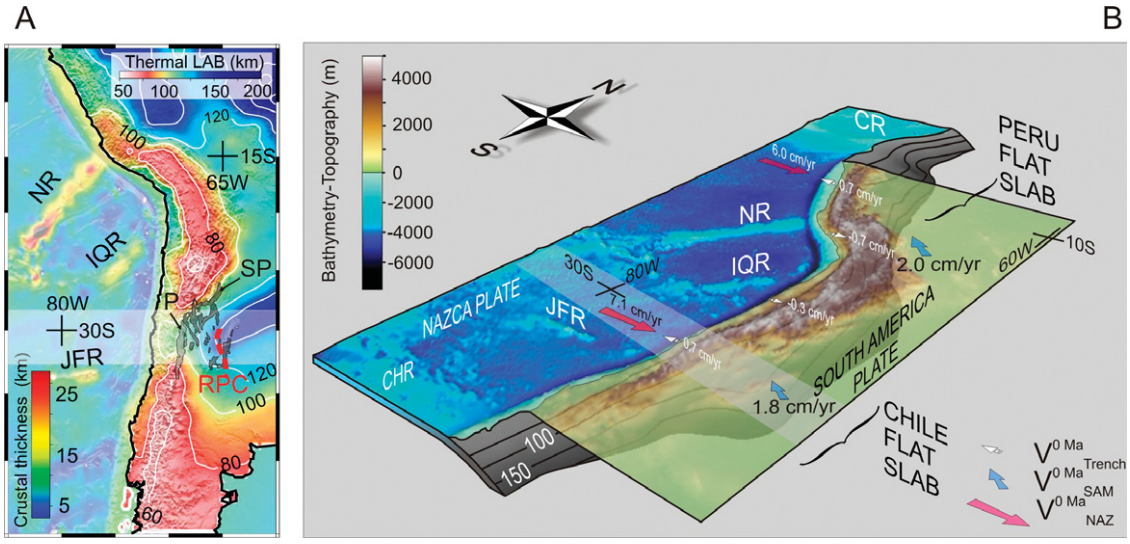

Figure 1. Relationship between observed data and subduction style along Andean subduction zone. A: Onshore: thermal lithosphere-asthenosphere boundary (LAB), defined as depth to 1300 °C (Tassara et al., 2006); flat subduction areas coincide with thick continental lithosphere. Red dashed line indicates western extent of Rio de la Plata craton (RPC), estimated to be ≥200 km thick from magnetotelluric studies (Booker et al., 2004; Favetto et al., 2008). SP—Sierras Pampeanas (dark gray), P—Precordillera (light gray). Offshore: oceanic crustal thickness derived from gravity modeling (Tassara et al., 2006). IQR—Iquique Ridge, JFR—Juan Fernandez Ridge, NR—Nazca Ridge. B: Three-dimensional view of Nazca and South American plates showing contours of depth in kilometers to Wadati-Benioff zone (Syracuse and Abers, 2006). Red, blue, and white arrows are present plate velocities (V) along the Peru-Chile Trench and of Nazca (NAZ) and South American (SAM) plates in Indo-Atlantic hotspot reference frame. East-west transparent bar shows modeled area. CR—Carnegie Ridge, CHR—Chile Ridge.

*E-mail: vlad@geociencias.unam.mx; vlad_manea@yahoo.com.

Carnegie, Cocos (Michaud et al., 2009), and Tehuantepec Ridges (Manea and Manea, 2008).

Flat subduction may also result from an increase in the nonhydrostatic pressure forces related to subduction driven flow within the asthenospheric wedge (Stevenson and Turner, 1977). The latter force, known as suction, acts toward preventing the slab from sinking into the mantle. Suction increases with subduction velocity, narrowness, and viscosity of the mantle wedge (Stevenson and Turner, 1977; Manea and Gurnis, 2007), but the effect of variations in the shape of the mantle wedge generated by the varying thickness of the overriding lithosphere has not been considered. This may be important in South America and in the Cenozoic subduction of North America, where cratons are or were located relatively close to a trench (Pérez-Gussinyé et al., 2008; Humphreys, 2009) (Fig. 1). O'Driscoll et al. (2009) found that a 250-km-thick cratonic root 300 km away from the trench resulted in twice the suction force compared to a rootless model. However, because they did not model the time evolution of subduction they could not demonstrate whether this would result in slab flattening.

The trenchward motion of South America has also been proposed to promote flat subduction (van Hunen et al., 2004), but why it develops only in some areas is not clear. Here we show time-dependent numerical experiments, which for the first time explore the influence of both the overriding plate thickness and trench motion on the subduction angle.

NUMERICAL MODELING STRATEGY AND RESULTS

Our numerical experiments are designed to reproduce the development of the Chilean flat subduction zone, where the geometry of the slab (Alvarado et al., 2009) and temporal and spatial evolution of volcanism (Ramos et al., 2002; Kay and Abbruzzi, 1996) are relatively well known (see the GSA Data Repository[1]). We use a three-dimensional (3-D) finite element model for a spherical domain (Tan et al., 2006), with the following boundary conditions: top and bottom boundaries are isothermal, and the lateral boundaries are reflective, the top boundary has an imposed velocity boundary condition, the bottom is free slip, and the sides are reflecting (Fig. DR2 in the Data Repository). In our experiments, we systematically varied the initial distance from trench to craton, d_{cr}^{ini}, and its thickness, h_{cr}, to accommodate uncertainties in these parameters (Fig. 2A; the final results of all experiments are in Fig. DR3). The value of h_{cr} varies between 150 km and 350 km, within the range of magnetotelluric (Booker et al., 2004; Favetto et al., 2008) and conductive lithosphere thickness estimates (Tassara et al., 2006) for the Rio de la Plata craton. Parameters like plate age (Sdrolias and Müller, 2006), surface plate velocities (Schellart et al., 2007), Andean shortening and trench erosion rate (Kley and Monaldi, 1998), and the extent of the low-viscosity wedge are relatively well known, considered to be constraints, and are kept constant. Note that inclusion of trench erosion and Andean shortening leads to differing trench and continent velocities, and that the trench in the flat slab area in Chile has been retreating for the past 25 m.y. (Schellart et al., 2007), a key factor in our results. In these simulations we kept wedge viscosity to a constant reference value of 10^{20} Pa s, because it represents the threshold at which the slab decouples from the overriding plate when the upper plate does not have a craton, and best reproduces the slab geometry south of the flat slab, where the slab is steep and there is no craton (Fig. 1A). Our conclusions also hold for smaller wedge viscosities (Section 2.1 and Figs. DR5 and DR6 in the Data Repository). In our reference model we keep the same kinematic boundary conditions as above, but do not include a craton in the upper plate. This experiment shows a decrease in the entrance angle from 45° to 30°, but no flat subduction occurs (Fig. DR4A). Thus, the large trenchward velocity of the continent, combined with trench retreat, is not able to generate flat subduction.

When a craton is included in the upper plate, d_{cr}^{ini} and h_{cr} greatly influence the slab geometry (Fig. 2A; Fig. DR3). When the craton approaches the trench the suction increases and tends to flatten the slab. When the d_{cr}^{ini} is large, >1100 km, suction forces do not increase enough to generate flat subduction (Fig. DR3). Some combinations of h_{cr} and d_{cr}^{ini} generate flat subduction (Fig. 2A). In these cases, because the slab is retreating, the rate of wedge closure is relatively small so that the increase in suction forces, which flatten the slab, is larger than the dynamic backward push by the mantle flow in the wedge that tends to steepen it.

We have defined the parameters that best fit the Chilean flat subduction zone according to two criteria: the slab geometry, as given by the slab earthquake data (Booker et al., 2004), and the present distance of the Peru-Chile Trench to craton, ~800 km (present craton location at ~64°W; Favetto et al., 2008). To allow for variations along the flat subduction segment we consider a best-fitting distance of ~800 ± 100 km (Fig. 2A; Fig. DR3). Note that the final distance between trench and craton is not a simple function of d_{cr}^{ini} and the imposed surface velocities. When the advancing craton meets the flattening slab at depth, where the velocities are not prescribed, the craton is deformed and pushed backward (Movie DR2 in the Data Repository). Figures 2B–2D show the final geometries after 30 m.y. of evolution for 3 of the best-fit cases.

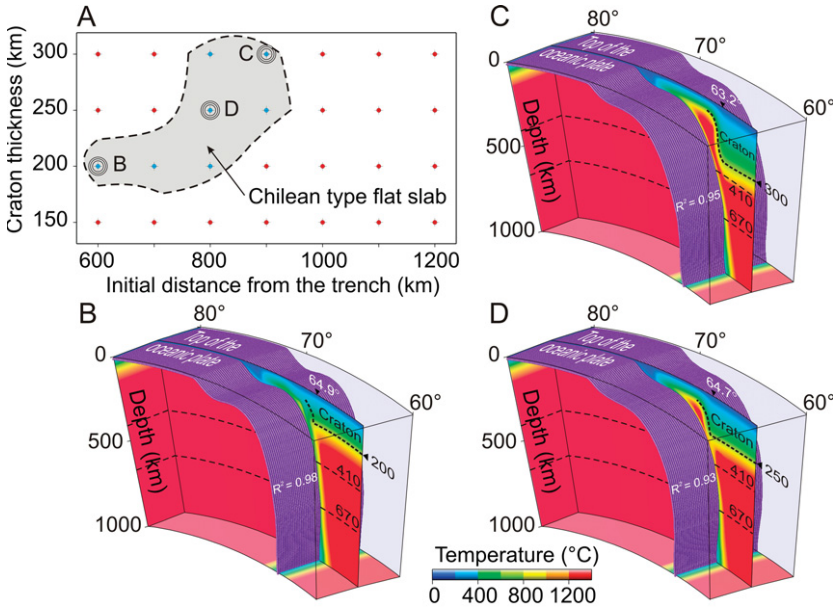

Figure 2. A: Domain diagram showing style of subduction as function of craton depth and initial distance from trench. Gray domain indicates models where slab geometry after 30 m.y. of evolution best fits present-day slab geometry and craton to trench distance (64°W ± 1°) in flat slab region of Chile. B, C, D: Temperature and geometry after 30 m.y. of evolution of three best-fitting models for flat slab domain in A. Dashed black lines represent craton shape; locations (in degrees; white lettering) of craton edge in each model are indicated.

[1]GSA Data Repository item 2012018, geodynamic modeling constraints, numeric modeling procedure and results, and supplementary figures and movies, is available online at www.geosociety.org/pubs/ft2012.htm, or on request from editing@geosociety.org or Documents Secretary, GSA, P.O. Box 9140, Boulder, CO 80301, USA.

SPATIAL AND TEMPORAL EVOLUTION OF UPPER PLATE DEFORMATION AND VOLCANISM

Figure DR4 shows the evolution of upper plate deformation for our reference model without a craton (A–C) and during slab flattening for one of our best-fit models (D–F). In our reference model, oceanic lithosphere subducts beneath thin continental lithosphere and the slab detaches from the upper plate and subducts at normal angles (Movie DR1). The negative pressure above the slab indicates the extent and magnitude of the suction; it is localized close to the trench and is smaller than the slab negative buoyancy (Fig. DR4B). In our best-fitting model, the negative pressure in the wedge is distributed along a wider segment of the slab, preventing it from sinking into the mantle and generating flat slab subduction (Fig. DR4E). In both cases the descending slab is in extension while the upper plate is in compression, in agreement with stress tensor orientations in the Chilean flat slab subduction zone (Alvarado et al., 2009; Fig. DR8). However, whereas in the reference model the upper plate maximum shear stress is concentrated close to the trench, in our flat slab model it is distributed over a much broader area further inland (Figs. DR4E and DR4F). Figure DR9A shows how the maximum shear stress in the upper plate migrates landward as the slab progressively flattens. The landward migration of the maximum shear stress in the upper plate starts from 20 to 15 Ma, which is consistent with broadening of deformation from the Cordillera Principal to the Precordillera during this period (Kay and Abbruzzi, 1996) (Fig. DR8). From 15 Ma the slab continues to flatten and the maximum shear stress region broadens further landward. By ca. 5 Ma, the maximum shear stress region extends as far as 65°W, which coincides with the location of the Sierras Pampeanas, where basement deformation occurred from ca. 5 to 2 Ma (Ramos et al., 2002). Upper plate compressional seismicity currently occurs in a broad area from the Precordillera to the Sierras Pampeanas (Ramos et al., 2002), in agreement with the area of maximum present shear stress in our best-fitting model (Fig. DR4F). Thus our modeling shows that slab flattening results in the development of compressional tectonics along hundreds of kilometers inland, as suggested for South American flat slabs (Ramos et al., 2002; Davila and Astini, 2007) and early Cenozoic compression in western North America (De Celles, 2004).

The best-fitting models also reproduce well the spatial and temporal evolution of volcanism in the Chilean flat slab (Ramos et al., 2002; Kay and Abbruzzi, 1996). Figure 3 shows the evolution of the temperature field and the wedge melting degree for one of our best fitting models. During the Early Miocene (20–15 Ma), the narrowing of the wedge has not yet affected volcanism, as inferred from observational studies (Ramos et al., 2002; Kay and Abbruzzi, 1996). By 12–10 Ma (Middle Miocene), flattening is underway, and the mantle wedge shrinks, resulting in broadening of the magmatic arc into the Precordillera. The maximum melting region in the wedge migrates eastward ~100 km (Fig. 3C), in accord with the recorded migration of the volcanic arc toward the Sierra Pampeanas (Ramos et al., 2002). The surface projection of the highest degree of wedge melting at 10 Ma in our model coincides with the location of volcanic activity for this period (Kay and Abbruzzi, 1996). The main shallowing phase takes place in our modeling ca. 5–6 Ma and is characterized by an eastward expansion of the magmatic front (Fig. 3C) and a further reduction in mantle wedge volume and temperature, which probably explains the cessation of volcanism at the Cordillera Principal and Precordillera between 7 and 6 Ma (Kay and Abbruzzi, 1996). The temperature in the wedge by 5 Ma is low enough to inhibit melting and subsequent volcanism, consistent with the observed cessation of magmatism by 4.7 Ma (Kay and Abbruzzi, 1996).

INFLUENCE OF TRENCH MOTION AND CONCLUSIONS

We have shown that the trenchward motion of normal thickness overriding lithosphere with velocities adequate for the Chilean flat slab area during the past 30 m.y., accompanied by trench retreat, is not enough to generate flat subduction in this area (Figs. 4A–4C). We speculate that steep subduction north and south of the Peru and Chilean flat slabs, respectively, where the Peru-Chile Trench retreated for the past 30 m.y., results from the absence of a craton sufficiently close to the trench (see Perez-Gussinye et al., 2008, their figure 6c). For the Chilean flat slab area we have found that only the combination of trenchward motion of thick cratonic lithosphere with trench retreat is able to reproduce the temporal and spatial evolution of slab flattening and its associated upper plate deformation and volcanism (Figs. 4D–4F). In addition, we have tested the trench motion influence on the development of flat subduction. Our models show that when the trench is stationary in time and space, the increase in suction due to craton trenchward motion and wedge closure is smaller than the dynamic backward push on the slab by the mantle in the narrowing wedge, and the slab does not flatten (Fig. DR7). We expect that this dynamic push will be larger in the case of trench advance (Figs. 4G–4I), and may explain the absence of flat subduction in the Bolivian orocline, where the Peru-Chile Trench has been nearly stationary or advanced little since 25 Ma (Schellart et al., 2007).

ACKNOWLEDGMENTS

All numeric computations were performed at the Computational Geodynamics Laboratory–CGEO (Centro de Geociencias, Campus Juriquilla, Queretaro, Universidad Nacional Autónoma de México) supercomputing facility (named Horus). We thank F. Davila, J. van Hunen, J. Martinod, and W. Schellart for comments that improved the paper, and R.F. Katz for generously sharing the code to calculate the equilibrium degree of melting in the mantle wedge. Financial support for this study was provided by

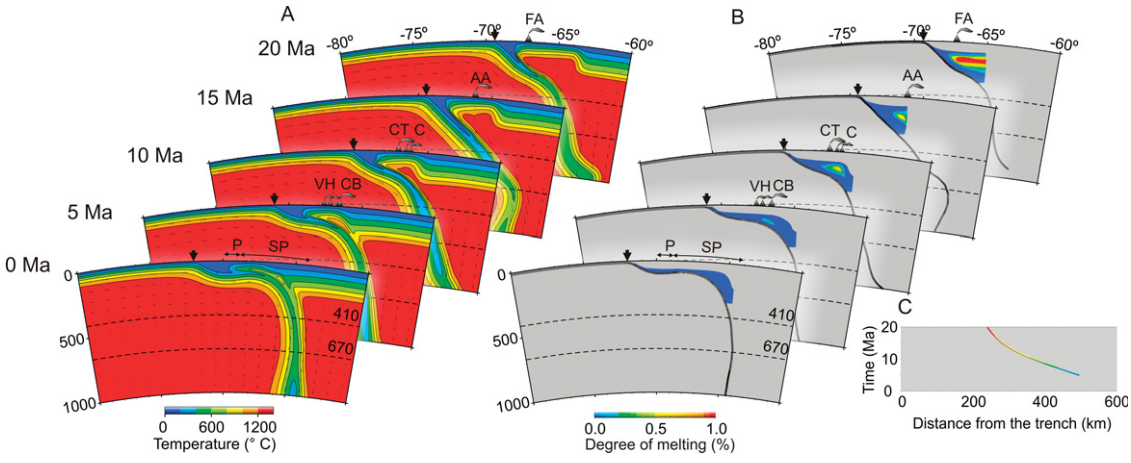

Figure 3. A: Evolution since Early Miocene of temperature field. B: Evolution since Early Miocene of degree of melting in mantle wedge. C: Distance from trench to surface projection of maximum mantle wedge melting for our best fitting model (Fig. 2B). During each time interval surface projection of model maximum degree of melting and highest mantle wedge temperature coincide well with locations of active volcanoes. FA—Farellones Arc, AA—Aconcagua, CT—Cerro de las Tortolas, C—Calingasta, VH—Vacas Heladas, CB—Cerro Blanco, P—Precordillera, SP—Sierras Pampeanas.

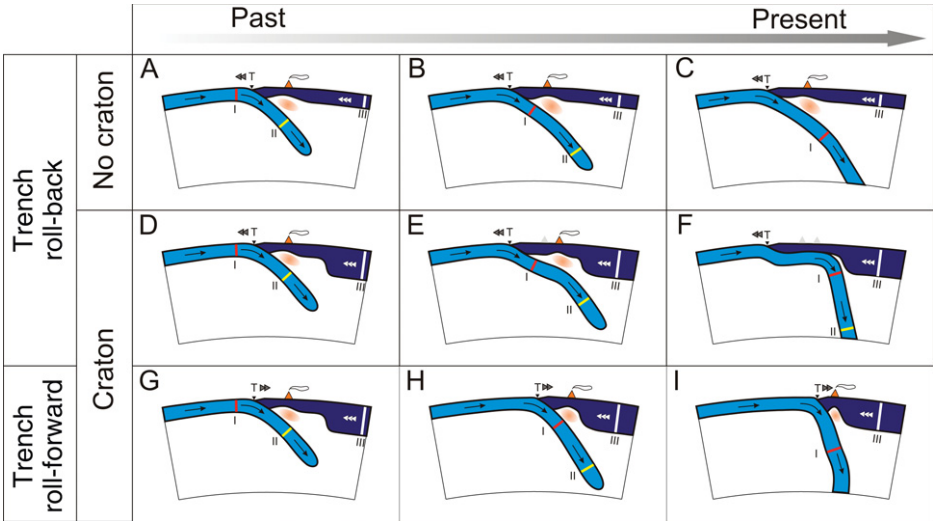

Figure 4. A–C: Conceptual models for evolution of subduction of oceanic lithosphere beneath trenchward-moving continent without a craton (CÑ craton; TÑ trench). D–F: Models for evolution of subduction of oceanic lithosphere beneath trenchward-moving continent with a craton. G–I: Models for evolution of subduction of oceanic lithosphere involving trench advance (continent with craton). Note that when there is a craton in upper plate and trench retreats, dynamic push is relatively small, due to diminished rate of wedge closure; result is that suction dominates and slab ßattens (DÐF). However, when trench advances (GÐI), dynamic push on slab surface will increase as rate of wedge closure increases, pushing slab backward and hindering slab ßattening.

Programa de Apoyo a Proyectos de Investigación e Innovación Tecnológica (PAPIIT) grants IN110709 and IN115810, and Consejo Nacional de Ciencia y Tecnología (CONACyT) grants 84035 and 117975.

REFERENCES CITED

Alvarado, P., Pardo, M., Gilbert, H., Miranda, S., Anderson, M., Saez, M., and Beck, S., 2009, Flat-slab subduction and crustal models for the seismically active Sierras Pampeanas region of Argentina, *in* Kay, S., et al., eds., Backbone of the Americas: Shallow subduction, plateau uplift, and ridge and terrane collision: Geological Society of America Memoir 204, p. 261–278, doi:10.1130/2009.1204(12).

Booker, J.R., Favetto, A., and Pomposiello, M.C., 2004, Low electrical resistivity associated with plunging of the Nazca flat slab beneath Argentina: Nature, v. 429, p. 399–403, doi:10.1038/nature02565.

Davila, F.M., and Astini, R.A., 2007, Cenozoic provenance history of synorogenic conglomerates in western Argentina (Famatina belt): Implications for Central Andean foreland development: Geological Society of America Bulletin, v. 119, p. 609–622, doi:10.1130/B26007.1.

DeCelles, P.G., 2004, Late Jurassic to Eocene evolution of the Cordilleran thrust belt and foreland basin system, western USA: American Journal of Science, v. 304, p. 105–168, doi:10.2475/ajs.304.2.105.

Favetto, A., Pomposiello, C., López de Luchi, M.G., and Booker, J., 2008, 2D magnetotelluric interpretation of the crust electrical resistivity across the Pampean terrane–Río de la Plata suture, in central Argentina: Tectonophysics, v. 459, p. 54–65, doi:10.1016/j.tecto.2007.11.071.

Gerya, T.V., Fossati, D., Cantieni, C., and Seward, D., 2009, Dynamic effects of aseismic ridge subduction: Numerical modelling: European Journal of Mineralogy, v. 21, p. 649–661, doi:10.1127/0935-1221/2009/0021-1931.

Gutscher, M.-A., Spakman, W., Bijwaard, H., and Engdahl, E.R., 2000, Geodynamics of flat subduction: Seismicity and tomographic constraints from the Andean margin: Tectonics, v. 19, p. 814–833, doi:10.1029/1999TC001152.

Humphreys, E., 2009, Relation of flat subduction to magmatism and deformation in the western United States, *in* Kay, S.M., et al., eds., Backbone of the Americas: Shallow subduction, plateau uplift, and ridge and terrane collision: Geological Society of America Memoir 204, p. 85–98, doi:10.1130/2009.1204(04).

Jarrard, R.D., 1986, Relations among subduction parameters: Reviews of Geophysics, v. 24, p. 217–284, doi:10.1029/RG024i002p00217.

Kay, S.M., and Abbruzzi, J.M., 1996, Magmatic evidence for Neogene lithospheric evolution of the Central Andean flat-slab between 30 and 32°S: Tectonophysics, v. 259, p. 15–28, doi:10.1016/0040-1951(96)00032-7.

Kley, J., and Monaldi, C.R., 1998, Tectonic shortening and crustal thickness in the Central Andes: How good is the correlation?: Geology, v. 26, p. 723–726, doi:10.1130/0091-7613(1998)026<0723:TSACTI>2.3.CO;2.

Manea, V.C., and Gurnis, M., 2007, Subduction zone evolution and low viscosity wedges and channels: Earth and Planetary Science Letters, v. 264, p. 22–45, doi:10.1016/j.epsl.2007.08.030.

Manea, M., and Manea, V.C., 2008, On the origin of El Chichón volcano and subduction of Tehuantepec Ridge: A geodynamical perspective: Journal of Volcanology and Geothermal Research, v. 175, p. 459–471, doi:10.1016/j.jvolgeores.2008.02.028.

Martinod, J., Funiciello, F., Faccenna, C., Labanieh, S., and Regard, V., 2005, Dynamical effects of subducting ridges: Insights from 3-D laboratory models: Geophysical Journal International, v. 163, p. 1137–1150, doi:10.1111/j.1365-246X.2005.02797.x.

Martinod, J., Husson, L., Roperch, P., Guillaume, B., and Espurt, N., 2010, Horizontal subduction zones, convergence velocity and the building of the Andes: Earth and Planetary Science Letters, v. 299, p. 299–309, doi:10.1016/j.epsl.2010.09.010.

Michaud, F., Wilt, C., and Royer, J.-Y., 2009, Influence of the subduction of the Carnegie volcanic ridge on Ecuadorian geology: Reality and fiction, *in* Kay, S.M., et al., eds., Backbone of the Americas: Shallow subduction, plateau uplift, and ridge and terrane collision: Geological Society of America Memoir 204, p. 217–228, doi:10.1130/2009.1204(10).

O'Driscoll, L.J., Humphreys, E.D., and Saucier, F., 2009, Subduction adjacent to deep continental roots: Enhanced negative pressure in the mantle wedge, mountain building and continental motion: Earth and Planetary Science Letters, v. 280, p. 61–70, doi:10.1016/j.epsl.2009.01.020.

Pérez-Gussinyé, M., Lowry, A.R., Phipps Morgan, J., and Tassara, A., 2008, Effective elastic thickness variations along the Andean margin and their relationship to subduction geometry: Geochemistry Geophysics Geosystems, v. 9, Q02003, doi:10.1029/2007GC001786.

Ramos, V.A., Cristallini, E.O., and Pérez, D.J., 2002, The Pampean flat-slab of the central Andes: Journal of South American Earth Sciences, v. 15, p. 59–78, doi:10.1016/S0895-9811(02)00006-8.

Schellart, W.P., Freeman, J., Stegman, D.R., Moresi, L., and May, D., 2007, Evolution and diversity of subduction zones controlled by slab width: Nature, v. 446, p. 308–311, doi:10.1038/nature05615.

Sdrolias, M., and Müller, D., 2006, Controls on back-arc basin formation: Geochemistry Geophysics Geosystems, v. 7, Q04016, doi:10.1029/2005GC001090.

Skinner, S.M., and Clayton, R.W., 2010, An evaluation of proposed mechanisms of slab flattening on central Mexico: Pure and Applied Geophysics, v. 168, p. 1461–1474, doi:10.1007/s00024-010-0200-3.

Stevenson, D.J., and Turner, S.J., 1977, Angle of subduction: Nature, v. 270, p. 334–336, doi:10.1038/270334a0.

Syracuse, E.M., and Abers, G.A., 2006, Global compilation of variations in slab depth beneath arc volcanoes and implications: Geochemistry Geophysics Geosystems, v. 7, Q05017, doi:10.1029/2005GC001045.

Tan, E. Choi, E., Thoutireddy, P., Gurnis, M., and Aivazis, M., 2006, GeoFramework: Coupling multiple models of mantle convection within a computational framework: Geochemistry Geophysics Geosystems, v. 7, Q06001, doi:10.1029/2005GC001155.

Tassara, A., Goetze, H.-J., and Hackney, R., 2006, Three-dimensional density modeling of the Nazca plate and the Andean continental margin: Journal of Geophysical Research, v. 111, B09404, doi:10.1029/2005JB003976.

van Hunen, J., van der Berg, A.P., and Vlaar, N.J., 2004, Various mechanisms to induce present-day flat subduction and implications for the younger Earth: A numerical parameter study: Physics of the Earth and Planetary Interiors, v. 146, p. 179–194, doi:10.1016/j.pepi.2003.07.027.

Manuscript received 9 June 2011
Revised manuscript received 2 August 2011
Manuscript accepted 16 August 2011

Printed in USA